Thin Solid Films 669 (2019) 558–563

Contents lists available at ScienceDirect

Thin Solid Films

journal homepage: www.elsevier.com/locate/tsf

Compositional correlation and polymorphism in BaF_2-PrF_3 thin films deposited using electron-beam evaporation

Weixiang He[a,c], Weimin Zheng[b], Ping Xie[c], Bin Li[c,*], Xuwen Lv[a,c], Chao Jing[a,*], Dingquan Liu[c,d]

[a] Department of Physics, Shanghai University, Shanghai 200444, China
[b] School of Space Science and Physics, Shandong University, Weihai 264209, China
[c] Shanghai Institute of Technical Physics, Chinese Academy of Sciences, Shanghai 200083, China
[d] School of Physical Science and Technology, Shanghai Tech University, Shanghai 200031, China

ARTICLE INFO

Keywords:
Infrared low-index evaporation materials
BaF_2-PrF_3
Electron beam evaporation
Compositional correlation
Polymorphism

ABSTRACT

Infrared low-index evaporation materials are essential in the broadband antireflection coatings to reduce Fresnel reflections on the surfaces of infrared optical components. Although the layers of praseodymium fluoride (PrF_3) show an excellent transparency and the lower refractive index *n* and extinction coefficient *k* in the spectral range of thermal infrared, the tensile stress presented in the layers prohibits PrF_3 from being used as infrared low-index coating materials. A practical solution to reduce stress is to directly evaporate the admixture of PrF_3 with alkaline fluorides, such as barium fluoride (BaF_2). However, due to the significant difference of vapor pressures between PrF_3 and BaF_2, it is commonly difficult to congruently deposit PrF_3-BaF_2 thin films utilizing evaporating directly from a single source. Moreover, more details are unknown about the phase compositions of PrF_3-BaF_2 thin films. In our investigation, BaF_2-PrF_3 thin films were deposited using electron beam evaporation from the sintered ingots of PrF_3 admixed with BaF_2. The compositions of thin films were characterized using energy dispersive X-ray spectroscopy (EDX), the crystallographic structures were explored by X-ray-diffraction (XRD). It was revealed that the concentration of BaF_2 in thin films can be correlated to that in the admixtures. Moreover, in addition to PrF_3 and BaF_2, the phase compositions in thin films include also secondary phases, such as PrOF, PrF_4, Pr_2F_2, $BaPrF_6$, and that of elemental Ba.

1. Introduction

The broadband antireflection coatings are indispensable for optical components, such as lens and windows, in the systems operating in the spectral range of thermal infrared, because they are commonly made of high-refractive-index materials. A typical solution to enhance the spectral transmittance of infrared optical components is to use a step-down index profile to match the refractive index of the substrate to the refractive index of the incident medium, the air in most of the cases. Therefore, the lowest value of refractive index available for an infrared-transmitting low-index coating material is critical to obtain the highest and broadest transmission zone [1].

Although thorium fluoride (ThF_4) is a mechanically stable infrared coating material with a low refractive index, special handling and strict disposal are required due to its radioactivity [2]. Some non-radioactive substitutions for ThF_4 are the rare-earth fluorides, such as ytterbium fluoride (YbF_3) and yttrium fluoride (YF_3) [3,4]. In our previous investigation, it has been revealed that PrF_3 can also be regarded as a potential infrared low-index material used in infrared antireflection to substitute for radioactive ThF_4, because its thin films have an excellent transparency, the lower refractive index *n* and extinction coefficient *k* in the spectral range of thermal infrared [5,6]. However, the layers of single rare-earth fluorides are known to appear with a high intrinsic tensile stress, which can induce the distortion of the substrate, cracks, and delamination in layers, peeling-off from the substrate, even the failure of the durability and optical performance [3,4,7,8].

An effective solution to reduce the more considerable stress in the layers of rare earth fluorides is to deposit the layers of rare earth fluorides admixed with some alkaline earth fluorides [9,10]. In our recent investigation, a new infrared low-index evaporation material, PrF_3 admixed with BaF_2, was developed. It can be observed that stress in BaF_2-PrF_3 thin films is reduced with the increase of the concentration of BaF_2. Moreover, it was also indicated that the unique optical properties of PrF_3 thin films, such as good transparency, the lower refractive index *n* and extinction coefficient *k* in the spectral range of thermal infrared, were presented [11].

* Corresponding author.
E-mail addresses: binli@mail.sitp.ac.cn (B. Li), cjing@staff.shu.edu.cn (C. Jing).

https://doi.org/10.1016/j.tsf.2018.11.056
Received 29 March 2018; Received in revised form 27 November 2018; Accepted 27 November 2018
Available online 28 November 2018

Interpretation of the optical and mechanical properties of BaF_2-PrF_3 thin films without detailed knowledge of the real crystallographic structure is incomplete because the phase compositions emerging in thin films have a strong influence on their properties. Moreover, although it has been a long history to deposit a layer and to modify its stress by evaporating simultaneously two substances from two sources, it may be desirable from a practical viewpoint to use a single source because of its simplicity, controllability and relatively low cost [12]. A great hindrance to achieving the single source evaporation exists related with the more considerable difference of vapor pressures between rare earth fluorides and alkaline earth fluorides, which results into vapor compositions in the chamber usually different from the proportion in original evaporants. As a consequence, the compositions in thin films deposited are generally different from those in evaporants.

In the investigation presented here, we are concerned with various problems involved in the compositional correlation and the phase compositions of BaF_2-PrF_3 thin films deposited using electron beam evaporating directly from the sintered ingots of admixtures of PrF_3 and BaF_2.

2. Experimental details

Granulates (1–3 mm) of PrF_3 guaranteed to be 99.9% pure were commercially obtained from Hitop Industrial Co. Ltd., China, and powders of BaF_2 with a purity of 99.99% obtained from China New Metal Materials Technology Co., Ltd. They were weighed to yield the mixtures corresponding to nominal concentration ratios of $w = [BaF_2]/([BaF_2] + [PrF_3]) = 0.05, 0.10, 0.15, 0.20, 0.25, 0.30, 0.35, 0.40$ and 0.45. About 30 g of each mixture, accompanied with PrF_3 as a comparison, was introduced into a cylindrical agate container (7 cm deep, 7.5 cm inner diameter) containing 20 agate balls (0.8 cm diameter) in order to be mixed and ground thoroughly at a rotor speed of 400 rpm for 6 h on a XQM-2 L planetary ball miller. The loading and unloading of the mixtures into and from the containers were always done inside a nitrogen-filled glove box.

The powder blends were then axially compacted into the ingots with a one-inch diameter at room temperature with a pressure of 40 MPa using a DY-400 electric hydraulic pressing machine. The ingots were subsequently sintered in the inert atmosphere (purified argon or helium) by using a 300 °C/h heating rate followed by a 4 h heat treatment at 1000 °C and completed by a 500 °C/h cooling stage using a GSL-1100×-50-LVT tube furnace.

The obtained ingots were evaporated using a C6 four-pocket electron beam evaporator in a background vacuum 2.0×10^{-3} Pa in the chamber of a KD500 box coater. A beam current of around 20 mA at a voltage of 6 kV was reached, and a graphite line was used. A flat calotte was rotated at a rate of 30 rpm to provide a good uniformity of thin films. The double-side polished Ge (111) wafers with a diameter of 10 mm and a thickness of 0.8 mm were used as substrates. The substrates were heated by radiation heaters, and the temperature was sensed by a platinum resistance temperature transducer pressed directly against the upper surface of a substrate. The signals from the transducer were transferred out through a set of electric-brush and slip-ring to operate a temperature controller and thus maintained a constant temperature of 200 °C. The thicknesses of all of the thin films were kept at a constant of approximate 2 μm and controlled using an Inficon SQM-160 multi-film rate/thickness monitor.

The compositions of BaF_2-PrF_3 thin films were determined using the energy dispersive X-ray analysis (EDX) from a Horiba EX-220 energy dispersive X-ray microanalyzer (model 6853-H) attached to a Hitachi S-4300 cold field emission scanning electron microscope (FE-SEM) without coating the surfaces. Prior to the analysis, a calibration had been carried out to a sintered polycrystalline sample of magnesium fluoride (MgF_2). The measurements were performed on three samples in the same batch, and the average values and standard deviations of the concentrations of BaF_2 in thin films were extracted. A pattern of EDX spectrum was demonstrated in Fig. 1 for thin films deposited from the sintered ingot with the amounts of BaF_2 in the admixtures corresponding to $w = 0.10$. It can be confirmed that the element of oxygen and other traces related to contaminations cannot be detected. The traces corresponding to the element of germanium perhaps originated from the substrates; moreover, the element of copper probably originated from the sample holder used in the measurement.

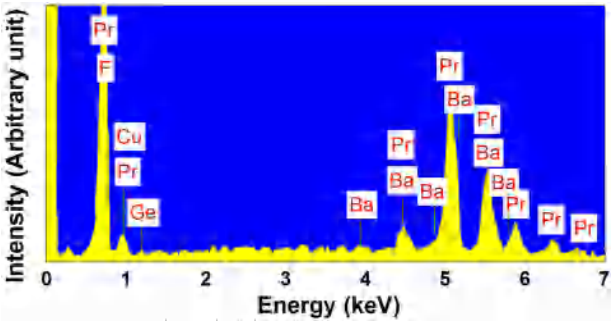

Fig. 1. A pattern of EDX spectrum for BaF_2-PrF_3 thin films deposited using e-beam evaporation from the sintered ingot with the amounts of BaF_2 in the admixtures corresponding to $w = 0.10$.

The phase compositions in BaF_2-PrF_3 thin films were examined by X-ray-diffraction (XRD) using a standard measurement from Cu K_α radiation on a Rigaku D/max 2550 V diffractometer in the range of 20–80° with an accuracy of 0.02°.

3. Results and discussion

3.1. Compositional correlation

From the results of measured compositions in BaF_2-PrF_3 thin films using EDX analysis, it was possible to calculate the concentration percentages of elements of Ba, Pr and F, designated as $x = [Ba]/([Ba] + [Pr] + [F])$, $y = [Pr]/([Ba] + [Pr] + [F])$, and, $z = [F]/([Ba] + [Pr] + [F])$, respectively. The results were summarized in Table 1.

Moreover, the concentration percentages of three elements, x, y, and z, were compared with the amounts of BaF_2 in the sintered ingots of admixtures corresponding to the nominal value of w, as illustrated in Fig. 2. As the guidelines for the eyes, the ideal concentration percentages of elements of Ba, Pr, and F, corresponding to the stoichiometric relationships, were also included within the figure and were presented with the black line, green line and pink line, respectively.

It can be revealed that the concentrations of the element of Ba in BaF_2-PrF_3 thin films are less than those corresponding to the ideal stoichiometric relationships; equivalently, the concentrations of the element of Pr in thin films are greater than those corresponding to the stoichiometric relationships. The differences of the concentrations of elements of Ba and Pr in thin films from those in the admixtures can be perfectly explained according to the difference of vapor pressures of PrF_3 and BaF_2 because PrF_3 has a much greater vapor pressure than that of BaF_2 [13,14]. However, the concentration of the element of Ba in BaF_2-PrF_3 thin films increases with the amounts of BaF_2 in the admixtures; moreover, the concentrations of the element of Pr in thin films decrease with the increase of the amounts of BaF_2 in the admixtures in an approximately linear manner. Therefore, for the convenience, the concentration ratios of $u = [Ba]/([Ba] + [Pr])$ can be used to designate the concentrations of BaF_2 in thin films.

In Fig. 3, the measured concentration ratios u in thin films (red ball) were presented. The error bars represent standard deviations of the concentrations of BaF_2 in thin films when measurements were performed on three independent samples in the same evaporation batch from an admixture. As a comparison, the stoichiometric relationship

Table 1
A summary of the concentration percentages, x, y, z, of elements Ba, Pr and F in BaF_2-PrF_3 thin films, accompanied with the concentration ratios, w, of BaF_2 in the admixtures and the ratios, u, of BaF_2 in thin films.

$w = \frac{[BaF_2]}{[BaF_2]+[PrF_3]}$ (Conc. ratio) in ingots	$x = \frac{[Ba]}{[Ba]+[Pr]+[F]}$ (Conc. %) in thin films	$y = \frac{[Pr]}{[Ba]+[Pr]+[F]}$ (Conc. %) in thin films	$z = \frac{[F]}{[Ba]+[Pr]+[F]}$ (Conc. %) in thin films	$u = \frac{[Ba]}{[Ba]+[Pr]}$ (Conc. ratio) in thin films
PrF_3	0	29.62	70.38	0
0.05	1.90	27.29	70.81	0.07
0.10	2.45	27.17	70.39	0.08
0.15	2.96	25.47	71.57	0.10
0.20	3.46	24.82	71.72	0.12
0.25	5.15	22.91	71.94	0.18
0.30	5.28	23.17	71.52	0.19
0.35	7.64	21.23	71.13	0.26
0.40	12.31	19.95	67.74	0.38
0.45	14.06	19.42	66.52	0.42

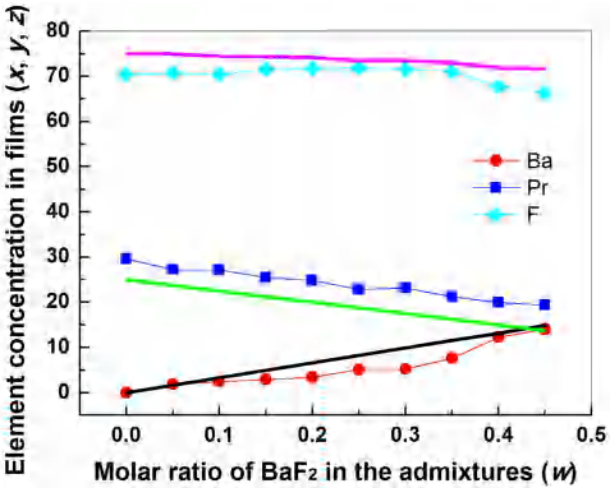

Fig. 2. A comparison of the concentration percentage, x, y, z, of elements Ba, Pr and F in BaF_2-PrF_3 thin films to the stoichiometric relationships.

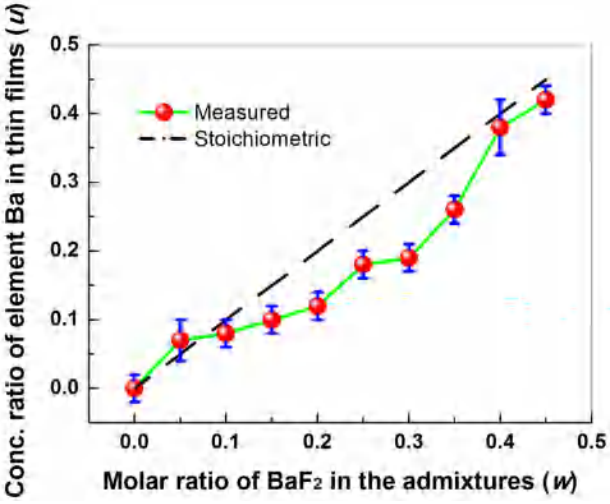

Fig. 3. The dependence of the concentration ratio u in thin films on the molar ratio of BaF_2 in the admixture w. The error bars represent standard deviations of the concentrations of BaF_2 in thin films measured on three independent samples in the same evaporation batch from an admixture.

was also included (black dotted line). It can be found that, therefore, although the deviations exist in BaF_2-PrF_3 thin films from the stoichiometric relationships, the concentrations of BaF_2 in thin films can be correlated with the nominal value w of BaF_2 in the admixtures.

In addition, it is worthwhile to note that all thin films of BaF_2-PrF_3 demonstrate characteristics of fluorine deficiency, which is likely to occur in thin films of fluorides prepared by electron beam evaporation without ion assistance. Since a molecular of BaF_2 has two fluorine atoms, while a molecular of PrF_3 has three, the number of fluorine atoms in the ideal stoichiometric relationship in thin films can be expressed in the form of $0.75(1\text{-}u) + 0.67u$, as designated as a pink line in Fig. 2. The difference between the fluorine atom concentrations in the ideal stoichiometric relationship and those fluorine atom concentrations measured can be illustrated in Fig. 4 with the increasing of the concentration ratios u in thin films. It can be shown that the concentrations of the element of F in thin films with the concentration ratios of the element of Ba, u = 0.18, 0.19 and 0.26, are approaching to the stoichiometric relationships.

3.2. Polymorphism

The patterns of XRD analysis were demonstrated in Fig. 5 for BaF_2-PrF_3 thin films with the concentration ratios in thin films u = 0.07, 0.08, 0.12, 0.18, 0.19, 0.26, 0.38 and 0.42, as well as for PrF_3 thin films. The samples of thin films were designated as 0, 007, 008, 012, 018, 019, 026, 038 and 042, respectively. A polycrystalline characteristic was presented in all of the thin films. It can be seen in Fig. 5(a), in which all of diffraction peaks were exhibited in the angular range of 20–80°, that all of the reflections emerge mainly in four angular ranges, those are, $24.0° < 2\theta < 31.0°$, $42.5° < 2\theta < 45.5°$, $50.0° < 2\theta < 54.0°$, and, $62.0° < 2\theta < 72.5°$. Therefore, the details of reflections can be demonstrated in Fig. 5(b), (c), (d) and (e),

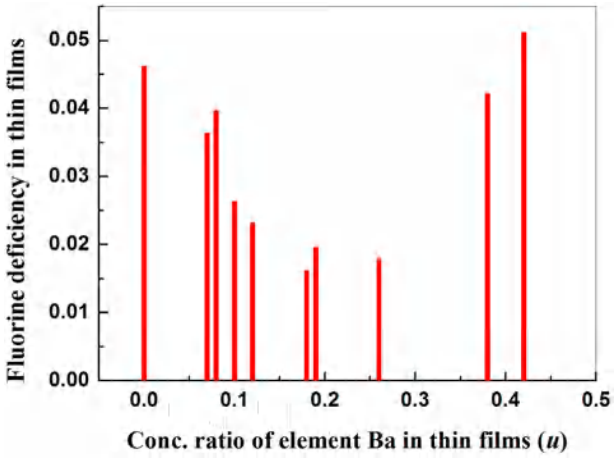

Fig. 4. The fluorine deficiency, designated as the difference between the fluorine atom concentrations in the ideal stoichiometric relationship and those measured, versus the concentration ratios u in thin films.

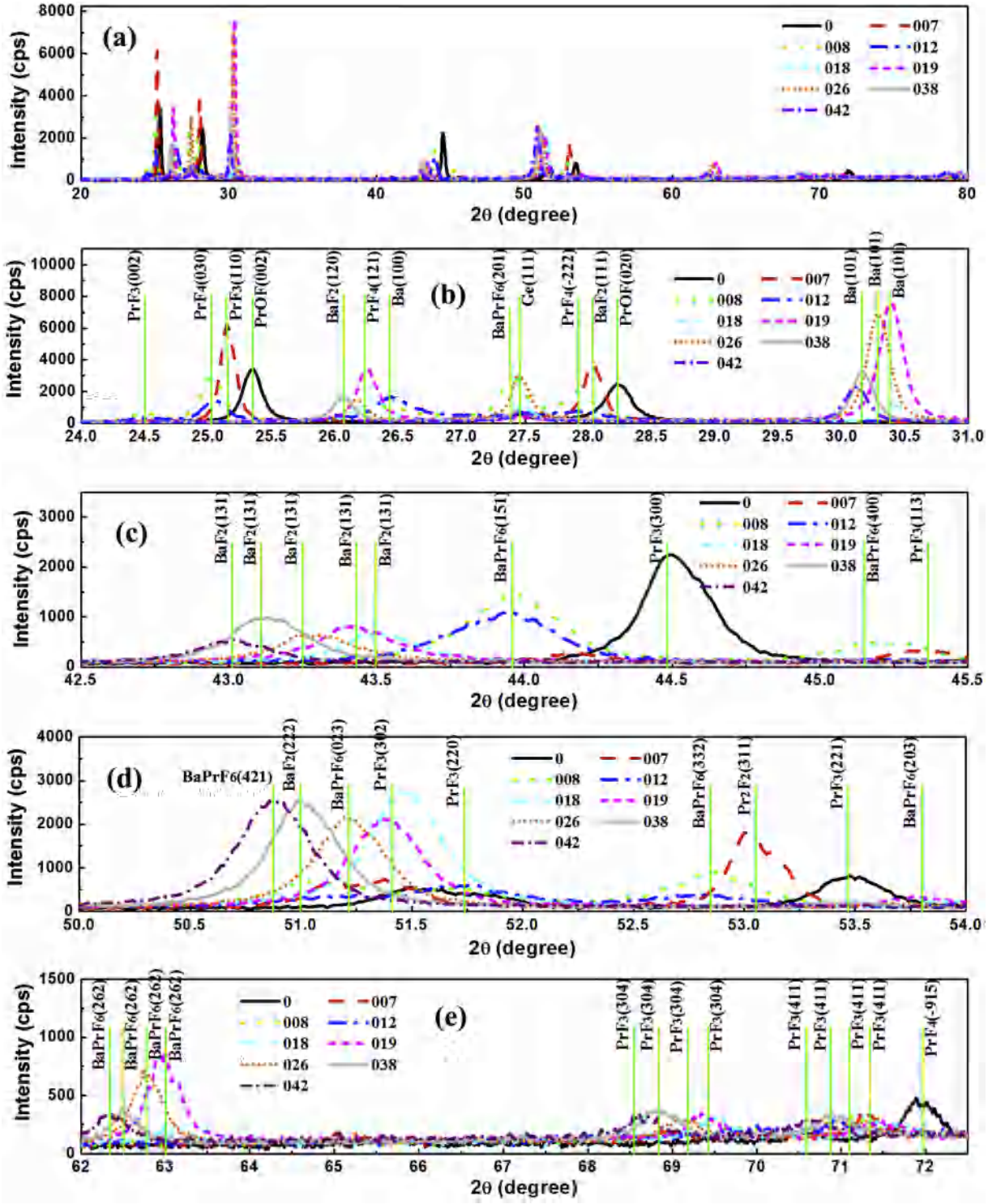

Fig. 5. The patterns of XRD analysis of PrF_3 and BaF_2-PrF_3 thin films with the concentration ratio u = 0.07, 0.08, 0.12, 0.18, 0.19, 0.26, 0.38 and 0.42, respectively. **(a).** all of diffraction peaks in the angular range of 20–80°, **(b).** an enlargement corresponding to the angular region of 24.0° < 2θ < 31.0°, **(c).** corresponding to the angular region of 42.5° < 2θ < 45.5°, **(d).** angular region of 50.0° < 2θ < 54.0°, **(e).** angular region of 62.0° < 2θ < 72.5°.

respectively.

It can be observed from the phase composition analysis that, the light green PrF_3 with a hexagonal structure (space group C_{3v}^3) corresponding to the JCPDS card number 46–1167, together with orthorhombic PrOF (space group D_{2h}^6) corresponding to the JCPDS card number 23–1386 and monoclinic PrF_4 (space group C_{2h}^6) corresponding to the JCPDS card number 30–1027, emerge in PrF_3 thin films. It is not surprised the occurrence of PrF_4 in PrF_3 thin films because among all of 17 rare-earth elements, Pr, together with Ce, Nd, Tb, and Dy, can be presented with a tetravalent state [15].

It has been commonly accepted that the majority of synthesized fluorides contains residual amounts of oxygen-containing phases, such as metal oxide fluoride, which demonstrates sparking of the melt, interaction with the evaporator in the process of evaporation in the vacuum. However, after admixing of PrF_3 with BaF_2 in the sintered ingots of admixtures, even if a concentration ratio as low as u = 0.07 was

Table 2
A summary of the phase compositions in BaF_2-PrF_3 thin films.

$u = \frac{[Ba]}{[Ba]+[Pr]}$ (Conc. ratio) in thin films	PrF_3	PrOF	PrF_4	BaF_2	Pr_2F_2	Ba	$BaPrF_6$
0	(300) (302) (221)	(002) (020)	(−915)				
0.07	(110) (113) (302) (411)			(111)	(311)		
0.08	(002) (411)		(030) (−222)	(222)		(100)	(201) (151) (400) (332)
0.12	(002) (220) (411)		(030) (−222)			(100)	(151) (332)
0.18	(302) (304)		(121)	(131)		(101)	(262)
0.19	(302) (304)		(121)	(131)		(101)	(203) (262) (304)
0.26	(304)		(121)	(131)		(101)	(023) (262)
0.38	(304) (411)			(120) (131) (222)		(101)	(262)
0.42	(304) (411)			(120) (131)		(101)	(421) (262)

presented in thin films, the thorough elimination of oxygen-containing phases can be carried out.

In BaF_2-PrF_3 thin films with a concentration ratio of BaF_2 of $u = 0.07$, the reflection emerges corresponding to the strongest diffraction peaks (111) of white BaF_2 with an orthorhombic structure (space group $D_{2h}{}^{16}$) to the JCPDS card number 34–0200. Furthermore, the reflection (311) can also be detected for the secondary phase of Pr_2F_2 with a cubic structure corresponding to the JCPDS card number 33–1074.

It can be revealed that three differences in phase composition exist between BaF_2-PrF_3 thin films with a concentration ratio $u = 0.08$ and thin films with a concentration ratio of $u = 0.07$. Firstly, the metallic precipitation emerges due to the diffraction peak (100) of elemental Ba, which has a hexagonal structure (space group $D_{6h}{}^{4}$) corresponding to the JCPDS card number 18–0148. Moreover, the secondary phase, $BaPrF_6$, presents in thin films, which has an orthorhombic structure (space group $D_{2h}{}^{21}$) corresponding to the JCPDS card number 38–1297. It is worthwhile to note that the Pr ions also present a tetravalent state in the secondary phase of $BaPrF_6$. Furthermore, the reflection corresponding to the secondary phase of Pr_2F_2 phase cannot be detected anymore. It is possible to explain these differences very well according to the phase diagram of the BaF_2-PrF_3 system. There exists a limited solubility of BaF_2 in PrF_3 at the PrF_3-rich phase boundary, where a solid solution of BaF_2 and PrF_3 is presented. Beyond this composition region, the phase composition of BaF_2 and PrF_3 coexist [16].

The phase composition in thin films with a concentration ratio $u = 0.12$ is similar to those with a concentration ratio $u = 0.08$, except that the reflection of BaF_2 cannot be detected. Moreover, the almost identical phase compositions exist also in thin films with the concentration ratios $u = 0.18$, 0.19 and 0.26, respectively, which have the preferred orientation of (101) corresponding to the strongest diffraction peaks of elemental Ba, instead of the preferred orientation of (100) presented in thin films with concentrations ratio $u = 0.08$ and 0.12. Besides, the almost identical phase structures are presented in thin films with the concentration ratios $u = 0.38$ and 0.42, respectively.

Furthermore, It can also be found that the obvious shifts of reflections toward a lower 2θ value are observed for PrF_3 (302) in BaF_2-PrF_3 thin films with the concentration ratios $u = 0.18$ and 0.19, respectively; for PrF_3 (411) in thin films with the concentration ratios $u = 0.07$, 0.08, 0.12, 0.38 and 0.42, respectively; for PrF_3 (304) in thin films with the concentration ratios $u = 0.18$, 0.19, 0.26, 0.38 and 0.42, respectively; for $BaPrF_6$ (262) with the concentration ratios $u = 0.19$, 0.26, 0.38 and 0.42, respectively; for BaF_2 (131) with $u = 0.18$, 0.19, 0.26, 0.38 and 0.42, respectively; for Ba (101) with $u = 0.19$, 0.26, 0.38 and 0.42, respectively. It is probably due to the ions doping into interstitial sites of those secondary phases, which enlarges the interlayer spacing. The phase compositions presented in BaF_2-PrF_3 thin films were summarized in Table 2.

4. Conclusions

In our investigation, it was founded that the concentrations of BaF_2 in thin films can be correlated to the concentration ratios of BaF_2 in the sintered ingots of admixtures. As a consequence, it can be carried out to deposit the BaF_2-PrF_3 thin films using electron beam evaporation directly from a single source, that is, a sintered admixture of PrF_3 and BaF_2. In addition, it also was disclosed that the addition of BaF_2 into PrF_3 can eliminate completely the oxygen-containing phase, such as PrOF, in the thin films.

In our further investigations, the influence of the occurrence of secondary phases on stress in thin films will be a subjects. Furthermore, the assessment the reliability and stability of thin films is in progress, which will demonstrate the comparative reliability and stability of the BaF_2-PrF_3 thin films as a potential candidate of infrared low-index evaporation material used in infrared antireflection to substitute for radioactive ThF_4.

Acknowledgments

This work is supported by the National Science Foundation of China (NSFC) under Grant No. 61675223 and Grant No. 51371111, Shandong Province Natural Science Foundation, China under Grant No. ZR2017MF018, Innovation Program in Shanghai Institute of Technical Physics, CAS, under Grant No. CX-173. Authors are grateful to Prof. X. M. Meng in Technical Institute of Physics and Chemistry, Chinese Academy of Sciences, for his help in performing the EDX analyzes, and to Dr. G. F. Cheng in Shanghai Institute of Ceramics, Chinese Academy of Sciences, for his assistance in completing the XRD analyzes.

References

[1] U.B. Schallenberg, Antireflection design concepts with equivalent layers, Appl. Opt. 45 (2006) 1507–1514.
[2] W. Heitmann, E. Ritter, Production and properties of vacuum evaporated films of thorium fluoride, Appl. Opt. 7 (1968) 307–309.
[3] V. Barrioz, S.J.C. Irvine, D.P. Jones, In situ and ex situ stress measurements of YF_3 single layer optical coatings deposited by electron beam evaporator, J. Mater. Sci. Mater. El. 14 (2003) 559–566.
[4] Y. Wang, Y.G. Zhang, W.L. Chen, W.D. Shen, X. Liu, P.F. Gu, Optical properties and residual stress of YbF_3 thin films deposited at different temperatures, Appl. Opt. 47 (2008) C319–C323.
[5] W.T. Su, B. Li, D.Q. Liu, F.S. Zhang, Texture evolution and infrared optical properties of praseodymium fluoride films, Opt. Mater. 30 (2007) 273–278.
[6] W.T. Su, B. Li, D.Q. Liu, F.S. Zhang, The determination of infrared optical constants of rare earth fluorides by classical Lorentz oscillator model, J. Phys. D. Appl. Phys. 40 (2007) 3343–3347.
[7] V. Barrioz, S.J.C. Irvine, D.P. Jones, In-situ stress monitoring with a laser-fiber system, Adv. Eng. Mater. 4 (2002) 550–554.
[8] W.D. Nix, Mechanical properties of thin films, Metall. Mater. Trans. A 20 (1989) 2217–2245.
[9] S.F. Pelllcori, Stress modification in cerous fluoride films through admixture with other fluoride compounds, Thin Solid Films 113 (1984) 287–295.
[10] J.D. Targove, A.R. Mupphy, Optical and structure characterization of mixed LaF_3-BaF_2 thin films, Thin Solid Films 191 (1990) 47–53.
[11] X.W. Lv, W.M. Zheng, P. Xie, B. Li, W.X. He, C. Jing, D.Q. Liu, Stress and optical constants in BaF_2-PrF_3 thin films deposited using electron-beam evaporation, Optik

173 (2018) 174–179.
[12] R.R. Willey, Practical design and production of optical thin films, Revised and Expanded, second ed., Marcel Dekker, New York, 2002.
[13] P.E. Hart, Vapor pressure and heat of sublimation of barium fluoride. Report No. UCRL-11124, Ernest O. Lawrence Radiation Laboratory, University of California, Berkeley, 1964.
[14] B.P. Sobolev, The Rare Earth Trifluorides. Pt.1. The high temperature chemistry of the rare earth trifluorides, Institut d'Estudis Catalanas, Barcelona, 2000.
[15] R. Hoppe, New fluorides with Ce^{IV}, Pr^{IV}, Nd^{IV}, Tb^{IV}, and Dy^{IV}, in: G.J. McCarthy, H.B. Silber, J.J. Rhyne (Eds.), The Rare Earths in Modern Science and Technology, Vol. 3, Plenam Press, New York, 1978, pp. 315–316.
[16] Acers-NIST, Phase equilibria diagrams, CD-ROM Database, Version 3.1.